Biochemical Pharmacology 80 (2010) 381–388

Contents lists available at ScienceDirect

Biochemical Pharmacology

journal homepage: www.elsevier.com/locate/biochempharm

The structure of the C-terminal helical bundle in glutathione transferase M2-2 determines its ability to inhibit the cardiac ryanodine receptor

Ruwani Hewawasam, Dan Liu, Marco G. Casarotto, Angela F. Dulhunty [1], Philip G. Board [1,*]

Structural Biology Program, John Curtin School of Medical Research, Australian National University, PO Box 334, Canberra, ACT 2601, Australia

ARTICLE INFO

Article history:
Received 19 January 2010
Accepted 15 April 2010

Keywords:
Glutathione transferase GSTM2-2
Cardiac RyR2 channels
Skeletal RyR1 channels
Calcium release from cardiac sarcoplasmic reticulum
Calcium release from skeletal sarcoplasmic reticulum
Lipid bilayer single channel experiments

ABSTRACT

Ca^{2+} release from the sarcoplasmic reticulum through cardiac ryanodine receptors (RyR2) is essential for heart function and is inhibited by the carboxy terminal domain of glutathione transferase M2-2 (GSTM2-C) and derivative fragments containing helix 6. Since a peptide encoding helix 6 alone does not fold into a helix and does not inhibit RyR2 Ca^{2+} release, the importance of the structure of helix 6 and its role in stabilizing GSTM2-C was tested by inserting potentially destabilizing mutations into this helical segment. GSTM2-C preparations with D156A or L163A mutations were so insoluble that the protein could not be purified. Proteins with F157A and Y260A substitutions were soluble, but had lost their capacity to inhibit both RyR2 Ca^{2+} release from vesicles and RyR2 channels in bilayers. Circular dichroism studies indicated that these mutated proteins retained their helical secondary structure, although changes in their endogenous tryptophan fluorescence indicated that the F157A and Y160A mutations caused changes in their folding. The single channel studies were conducted with 2 mM ATP and 10 μM Ca^{2+} in the cytoplasmic solution, mimicking concentrations in the cytosol of cardiac myocytes. Wild type GSTM2-C inhibited RyR2 only at a potential of +40 mV, which may develop during Ca^{2+} efflux, but not at −40 mV. Together, the results indicate that the structure of helix 6 in the C-terminal fold is critical to the inhibitory action of GSTM2-2 and suggest that therapeutics mimicking this structure may reduce excess Ca^{2+} release during diastole, which can lead to fatal arrhythmia.

1. Introduction

The ryanodine receptor (RyR) functions as an ion channel that releases Ca^{2+} from the sarcoplasmic reticulum (SR) and is essential for excitation contraction coupling and contraction in striated muscle. In previous studies we have shown that the human muscle specific glutathione transferase M2-2 (GSTM2-2) is a high affinity inhibitor of cardiac muscle ryanodine receptors (RyR2) and a weak activator of skeletal muscle ryanodine receptors (RyR1) [1,2]. Investigations of the function of endogenous modulators of RyR2 are important for understanding their contribution to cardiac output. In addition, inhibition of RyR2 is a potential strategy for the treatment of heart failure. The role of GSTM2-2 as an endogenous inhibitor of RyR2 is particularly important in the context of it helping to maintain low RyR2 activity during diastole. The cardiac RyR2 has few endogenous inhibitors and, unlike the skeletal RyR1, it is not sensitive to block by normal cytoplasmic concentrations of Mg^{2+} of around 1 mM [3,4]. It is essential that RyR2 activity is low during diastole so that Ca^{2+} concentrations are maintained at appropriate levels in the sarcoplasmic reticulum Ca^{2+} stores. It is well documented that excessively active RyR2 channels are partly responsible for low store Ca^{2+} levels and defective Ca^{2+} release in heart failure. Stress-induced ventricular arrhythmias linked to mutations in RyR2 (or its associated proteins) that cause the channels that remain active during diastole, can cause sudden death in apparently healthy young individuals [5].

We have explored the regions of GSTM2-2 that interact with RyR2 and inhibit the channel in the hope of finding a region that might be developed to reduce the activity of overly active RyR2 channels in heart failure and stress-induced arrhythmias. Cross linking studies have shown that GSTM2-2 binds to RyR2 through its C-terminal domain (GSTM2-C) and that this α-helical domain can independently inhibit RyR2 function but has no effect on skeletal muscle RyR1 Ca^{2+} channels [6]. Further dissection of GSTM2-C into a number of smaller peptides revealed that helix 6 is a core element that was essential for RyR2 inhibition. Previous studies [7] have shown that helix 6 plays a key role in global folding of the cytosolic GST family. However, we also found that a helix 6 peptide did not form an α-helix and was not an effective RyR2 inhibitor [6]. We have now made specific mutations in helix 6 within GSTM2-C to probe the relationship between helix 6 and the structure of GSTM2-C and its capacity to inhibit RyR2. The results provide further evidence for the importance of the stability

* Corresponding author. Tel.: +61 2 6125 4714; fax: +61 2 6125 4712.
E-mail address: Philip.Board@anu.edu.au (P.G. Board).
[1] Board and Dulhunty made equal senior author contributions to the manuscript.

0006-2952/$ – see front matter © 2010 Elsevier Inc. All rights reserved.
doi:10.1016/j.bcp.2010.04.019

of the structure of helix 6 in maintaining the inhibitory action of GSTM2-C.

2. Materials and methods

2.1. Reagents

The restriction enzymes were purchased from New England Biolabs (GENESEARCH PTY. LTD. 14 Technology Drive, Arundel, Queensland 4214 Australia), and T4 DNA ligase was from Promega (Suite W3A, Level 3, Westside Building, South Sydney Corporate Park, 75-85 O'Riordan Street, Alexandria NSW 2015). The *Pfu Turbo* DNA polymerase from Stratagene was used in polymerisation chain reactions (PCR). Plasmid purification kit and PCR fragment purification kit were from Qiagen (PO Box 641, Doncaster, VIC 3108). All other chemicals were purchased from Sigma–Aldrich Pty. Ltd (PO Box 970, Castle Hill, NSW 1765, Australia).

2.2. Expression and mutagenesis of recombinant GSTM2-C

Recombinant GSTM2-C was expressed in *E. coli* from a pHUE vector and purified by Ni-agarose affinity chromatography as previously described [6]. The poly His-ubiquitin tag used for the affinity chromatography was subsequently cleaved by digestion with a catalytic fragment of the deubiquitylating enzyme mouse Usp 2 [8]. This strategy provides recombinant GSTM2-C without any additional residues.

Mutagenesis was undertaken by overlapping PCR and the presence of the desired mutations and the absence of additional mutations was confirmed by DNA sequencing. The numbering of residues mutated in the C-terminal domain is based on the whole GSTM2 subunit.

2.3. Circular dichroism (CD)

The wild type GSTM2-2 and mutated forms were diluted to 1 mg/ml in 10 mM phosphate buffer and pH adjusted to 8.0. CD spectra were collected at 22 °C on a Chirascan CD spectrometer (Applied Photophysics Ltd, United Kingdom). Three spectra were collected, averaged and subjected to a smoothing function.

2.4. Fluorescence scanning

Experiments were performed on a LS50B Luminescence Spectrophotometer (Perkin Elmer, USA) using an excitation slit width of 10 nm and an emission slit width of 9 nm. Protein samples (5 μM) were placed in a quartz cuvette (Spectrosil Far UV quartz windows cuvette, Starna Cells Inc., USA) and the fluorescence signal was measured by exciting the sample at 280 nm and monitoring the emission at 290–450 nm. The maximum emission fluorescence intensity was observed at 340 nm.

2.5. Preparation of SR vesicles

Cardiac SR was prepared from sheep heart [9,10]. Vesicles were frozen and stored either in liquid N_2 or at −70 °C. Skeletal SR was isolated from the back and leg muscles of New Zealand White rabbits, and heavy SR was collected from the 35–45% (w/v) interface of a discontinuous sucrose gradient, centrifuged and resuspended [1,2,11–13].

2.6. Ca^{2+} release from SR

The methods for measuring Ca^{2+} release have been described previously [14,15] and are illustrated in Fig. 3 below. A Cary 3 spectrophotometer was used to monitor extravesicular Ca^{2+} at 710 nm, using the Ca^{2+} indicator antipyrylazo III. Cardiac SR vesicles (100 μg/ml) were added to a solution containing 100 mM KH_2PO_4, 0.4 mM antipyrylazo III, 1 mM Na_2ATP and 4 mM $MgCl_2$ controlled at a temperature of 25 °C and magnetically stirred. Cardiac SR vesicles were added to the cuvette, causing an increase in [Ca^{2+}] which then declined as Ca^{2+} was taken up by the Ca^{2+}-ATPase which was activated by the MgATP in the solution. The SR was then loaded with four additions of 7.5 μM Ca^{2+} (30 μM total). Thapsigargin (2.25 μM) was added to block the Ca^{2+}-ATPase, and then 5 mM caffeine to initiate Ca^{2+} release from the SR. Ruthenium red was added to confirm that Ca^{2+} release was through the RyR and finally Ca^{2+} ionophore (A23187) was added to release Ca^{2+} remaining in the SR and to demonstrate that that the antipyrylazo was not saturated with Ca^{2+} during the caffeine-induced release through RyR2. The SR vesicles were incubated for 20 min prior to the start of the experiment with the GSTM2-2 construct in vehicle buffer or with vehicle buffer alone for control experiments. The same concentrations of GSTM2-C construct in vehicle buffer or with vehicle buffer alone were added to the cuvette solution prior to vesicle addition. Calibration curves of optical density changes with four additions of 12.5 μM $CaCl_2$ to the cuvette solution (above) were constructed in the presence of vehicle or GSTM2-2 constructs and other compounds. None of the proteins, or the presence of caffeine or ruthenium red, affected the calibration curve. The baseline rate of Ca^{2+} release after addition of thapsigargin (slope b, Fig. 3B) and the initial rate of caffeine-induced Ca^{2+} release (slope a, Fig. 3B) were measured. An ATP regenerating system was not used. Since the protocol followed in these experiments was tightly controlled, the ATP concentration would have been the same during drug exposure in each experiment, and ATP would have been utilized at the same rate and varying with time in the same way from experiment to experiment. Since the rate of Ca^{2+} uptake during loading was the same in the first and fourth loading step (Fig. 3A) we assume that ATP was not severely depleted.

2.7. Single channel activity

Artificial lipid bilayers separating *cis* and *trans* solutions were formed across an ~100 μM hole in a delrin cup [1,2,12,13]. Single channel parameters were obtained using the Channel 2 program (developed by P.W. Gage and M. Smith, John Curtin School of Medical Research, Canberra, Australia). In general channels incorporated with their cytoplasmic surface of the SR facing the *cis* solution and this was confirmed by characteristic changes in channel activity with changes in cytoplasmic ATP and Ca^{2+} concentration in the *cis* chamber. For channel incorporation, the solutions were *cis*: 230 mM Cs methanesulphonate ($CsCH_3O_3S$), 20 mM CsCl, 1 mM $CaCl_2$, and 10 mM N-tris[hydroxymethyl]-methyl-2-aminoethanesulfonic acid (TES, pH 7.4); and *trans*: 30 mM $CsCH_3O_3S$, 20 mM CsCl, 1 mM $CaCl_2$, and 10 mM TES (pH 7.4). After channel incorporation, *cis* Ca^{2+} was reduced to 10 μM by perfusion with *cis* solution: 230 mM CsMS, 20 mM CsCl, 1.9 mM $CaCl_2$, 2 mM BAPTA; 10 mM TES. The Ca^{2+} concentration was confirmed using a Ca^{2+} electrode. *trans* [Cs^+] was raised to 250 mM with addition of 200 mM $CsCH_3O_3S$. Experiments were carried out at 23 ± 2 °C. Bilayer potential is expressed as the voltage in the cytoplasmic solution relative to luminal solution and was changed every 30 s between +40 mV and −40 mV. Current was recorded continuously throughout the experiment at 5 kHz and was filtered at 1 kHz. The open probability (P_o) was measured using either a threshold discriminator (when one channel only opened) or from mean current, I' (when bilayers contained more than one active channel). For threshold detection, a threshold was set outside the noise at ~20% of the maximum open conductance. Currents exceeding the threshold were detected as channel openings. The

mean current (I') is the average of all data points in a record. Relative I' is approximately equal to relative P_o and all data is given as relative P_o. The Ca^{2+} release record in Fig. 3A shows that the cardiac SR contains a substantial Ca^{2+} pool that does not respond to caffeine and is due to the presence of longitudinal SR, which lack RyR channels, but contains K^+ and Cl^- channels. Such channels were not seen in lipid bilayer experiments that were performed in the presence of $CsCH_3O_3S$ (K^+ channels are impermeable to Cs^+, and Cl^- channels are impermeable to $CH_3O_3S^-$). All channels were blocked by ruthenium red at the end of the experiment to confirm that they were RyR channels.

2.8. Statistics

Average data are given as mean ± SEM. Statistical significance was evaluated using paired or unpaired Student's *t*-test as appropriate or ANOVA. Numbers of observations (n) are given in Tables and Figure legends. For data shown in Figs. 4 and 5, bilayers occasionally broke after addition of either 5 or 15 μm of protein, so that additional experiments were performed with addition on only 30 μm of protein. Thus there were separate sets of control data for each concentration of protein, necessitating the use of ANOVA and the Mahalanobis test. To reduce effects of variability in control open probability (P_oc), and to evaluate test parameters after protein addition (P_ot), data were expressed as the difference between the $\log_{10} P_o$c and $\log_{10} P_o$t for each channel (e.g. $\log_{10} P_o\text{c} - \log_{10} P_o\text{t}$). The difference from control was assessed with a paired *t*-test applied to $\log_{10} P_o$C and $\log_{10} P_o$F. The difference between each concentration was assessed using ANOVA on $\log_{10} P_o\text{c} - \log_{10} P_o\text{t}$ at each concentration with the multidimensional Mahalanobis test. The difference between $\log_{10} P_o\text{c} - \log_{10} P_o\text{t}$ at +40 mV and at −40 mV at each concentration was assessed using the Student's *t*-test. A P value of <0.05 was considered significant for all tests.

3. Results

GSTM2-C consists of the 130 C-terminal residues of GSTM2 (residues 89–218) and based on the crystallographic structure of the complete GSTM2-2 molecule it is thought to contain helices 4–8. In previous studies we tested a number of fragments derived from GSTM2-C and found that only fragments containing helix 6 were able to inhibit RyR2 Ca^{2+} channels [6]. In addition, our previous data indicated that the capacity of GSTM2-C to inhibit RyR2 was not contained within a non–helical peptide derived from helix 6 and may be dependent helix 6 retaining its helical structure and/or stabilizing the overall fold of GSTM2-C. It is evident from the X-ray crystallographic structure of GSTM2-2 [16] that α-helix 6 forms the hydrophobic core of this domain and is surrounded by helices 4, 5, 7 and 8. Helix 6 is connected to the surrounding helices through a series of ionic and hydrophobic interactions (Fig. 1A). Indeed, helix 6 is more exposed in the GSTM2-C construct (Fig. 1B) which is more effective than the full-length construct in inhibiting RyR2. This configuration suggests that helix 6 is important for

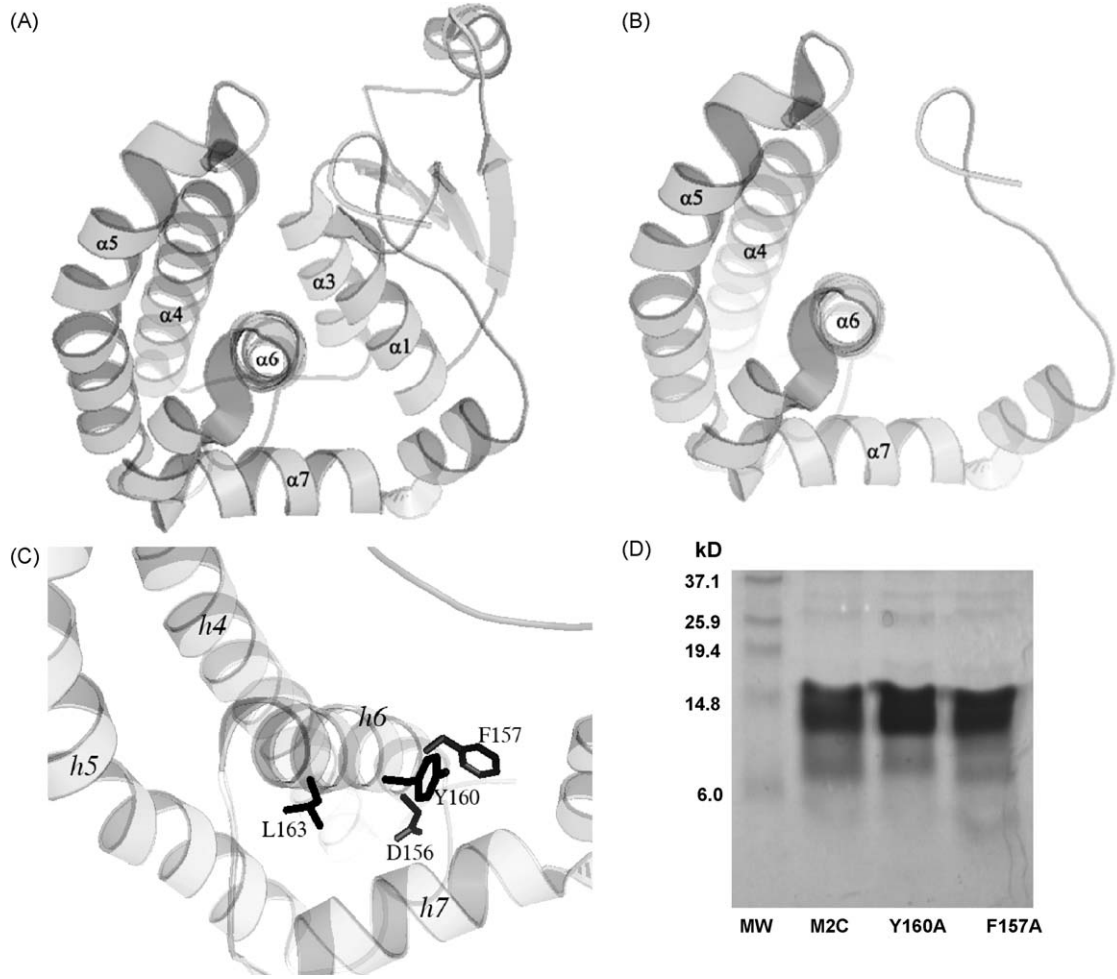

Fig. 1. The central location of a helix 6 in GSTM2 and GSTM2-C. (A) The crystal structure of GSTM2 from PDB file 1XW5. (B) The predicted structure of GSTM2-C after the removal of the N-terminal domain. (C) The position of the mutations F157A, L156, Y160A and L163A in helix 6 of GSTM2-C. The figure was prepared from the structural coordinates in PDB 1XW5. (D) SDS PAGE of purified recombinant GSTM2-C variants.

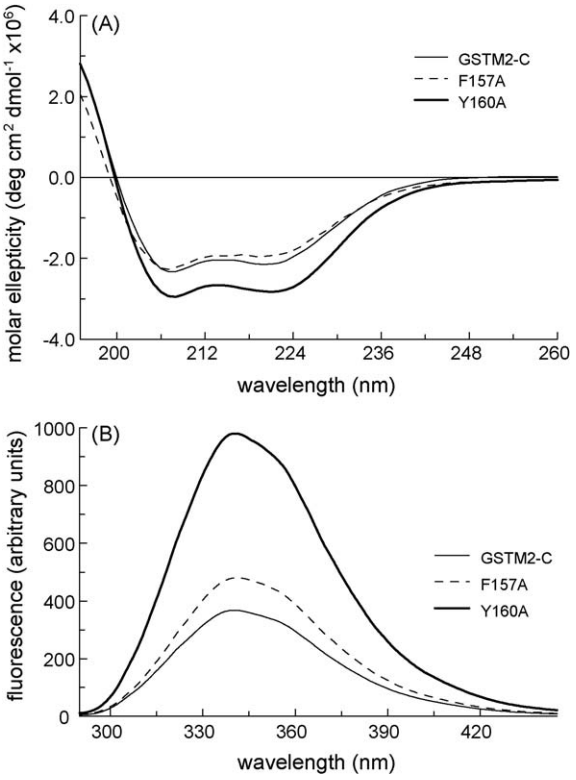

Fig. 2. Characterisation of GSTM2-C constructs. (A) Circular dichroism spectra for GSTM2-C and the mutated variants F157A and F160A. (B) The intrinsic tryptophan fluorescence spectra for GSTM2-C and the mutated variants F157A and F160A.

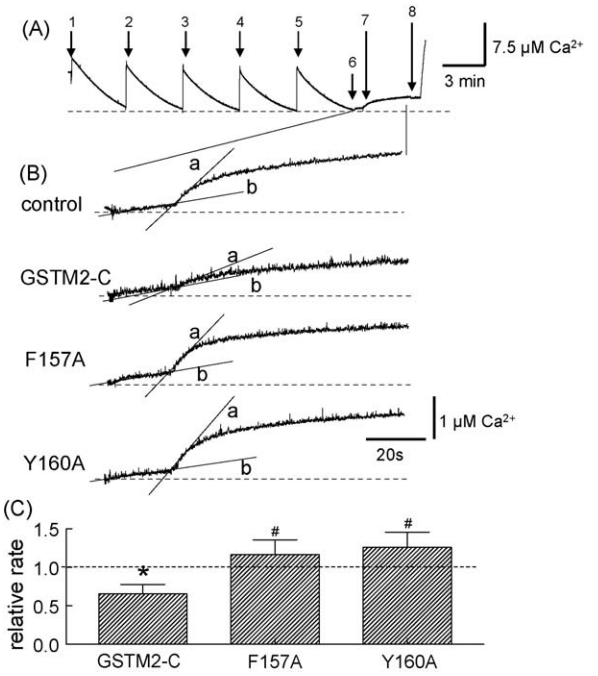

Fig. 3. Mutation of GSTM2-C prevents the protein from depressing the release of Ca^{2+} from the SR through RyR channels. (A) Full Ca^{2+} release experiment in which skeletal SR B4 vesicles were equilibrated with either 30 μM GSTM2-C construct or equivalent volume of vehicle for 20 min before addition to the cuvette solution also containing the 30 μM GSTM2-C construct or equivalent volume of vehicle (see Section 2). The recordings show optical density as a function of time after vesicle addition. An increase in optical density indicates an increase in extravesicular [Ca^{2+}] detected by antipyrylazo III absorbance at 710 nm. Cardiac SR vesicles were added to the cuvette at arrow 1. The [Ca^{2+}] increased with vesicle addition and then fell as the Ca^{2+} was taken up into the vesicles upon activation of the SR Ca^{2+}-ATPase by MgATP in the cuvette solution. The SR was then loaded with four additions of 7.5 μM Ca^{2+} (30 μM total) (arrows 2–5). Thapsigargin (2.25 μM) was added (arrow 6) to block the Ca^{2+}-ATPase, and then caffeine (5 mM) (arrow 7) to activate ryanodine receptors. Ruthenium red was added (arrow 8) followed by the Ca^{2+} ionophore which allowed Ca^{2+} remaining in the vesicles to equilibrate with the extravesicular solution (final large increase in [Ca^{2+}]). Block of Ca^{2+} release with ruthenium red verified that the caffeine-induced Ca^{2+} release was through RyR2. The final large increase in [Ca^{2+}] indicates (a) that Ca^{2+} had not been maximally released from the vesicles and (b) the antipyrylazo response was not saturated. (B) X and Y expansion of the baseline release in thapsigargin and the caffeine release transient (between arrows 6 and 8 in panel A). Shown are the transients with the vehicle alone (without a GSTM2-C construct, control – upper panel), the wild type GSTM2-C (second panel), F157A (third panel) and Y160A (lower panel). The line labeled (b) indicates the baseline Ca^{2+} release rate after addition of thapsigargin, while the line labeled (a) indicates the initial rate of Ca^{2+} release after caffeine addition. The lines are included to indicate where the measurement was taken. The rate was calculated from the derivative of the points in that region of the curve. (C) Average data showing caffeine-stimulated Ca^{2+} release rate in the presence of 30 μM GSTM2-C construct relative to the Ca^{2+} release rate in the presence of vehicle alone. The * symbol indicates a significant difference from control, the # symbols indicate that the F157A and Y160A data is significantly different from the wild type data.

maintaining the fold of the C-terminal domain and that the fold may be responsible for the inhibition of RyR2. To test this possibility, we aimed to disrupt key contacts between the α-6 helix and surrounding helices, and monitor the effects of these mutations on the structure of GSTM2-C and its capacity to inhibit Ca^{2+} release from cardiac SR and RyR2 Ca^{2+} channel activity.

Examination of the crystallographic structure of the entire GSTM2 protein (RCSB-1XW5), identified four residues within helix 6 that were in close proximity (<5 Å) to partner amino acid residues located in helices 5, 7 and 8, thereby potentially participating in hydrogen-bond, electrostatic or hydrophobic interactions. Four modified GSTM2-C proteins were produced by mutating each of the selected residues (Y160; F157; L163; D156) to an alanine residue with the specific aim of disrupting these contacts. Fig. 1C displays the ribbon structure of the C-terminal domain with the position of all mutated residues highlighted. The D156A and L163A mutants could not be successfully expressed in a soluble form, confirming that the conformation of the helix 6 is a key element in the folding and hence the stability of the C-terminal domain. However, the Y160A and F157A mutants were successfully purified for further study (Fig. 1D).

3.1. The effect of the F157A and Y160A mutations on protein structure

Circular dichroism spectra were obtained for each protein to determine if the mutations caused an alteration in the secondary structure. The spectra for the two mutant proteins are compared with the spectrum obtained from the unchanged GSTM2-C protein in Fig. 2A. Although the F257A and Y160A mutant proteins show a slightly more pronounced minima at 208 and 222 nM that may indicate a very slightly increased degree of helicity, the overall comparison suggests that the mutations have not caused a significant change in the overall secondary structure. To investigate if the mutations caused a change in the protein fold we compared the intrinsic tryptophan fluorescence spectra for these proteins (Fig. 2B). While both mutant proteins showed a distinct increase in fluorescence at 340 nm the increase with the Y160A mutant was particularly striking. These changes in tryptophan fluorescence emission suggest that both mutations have caused changes in the protein conformation that have altered the accessibility and environment of tryptophan residues that occur at position 146 in helix 5 and 214 at the C-terminal end of helix 8.

3.2. Effects of wild type and mutant GSTM2-C on Ca^{2+} release from SR vesicles

As previously shown [6] when 30 μM of the wild type GSTM2-C protein was added to cardiac muscle SR vesicles it causes a

Table 1
Rates of unstimulated Ca^{2+} leak after addition of thapsigargin, calculated from slope b (Fig. 3B) under control conditions and with the wild type and mutant GSTM2-2.

	Release rate in the presence of thapsigargin (pmol/mg/min)			
	Control $n=16$	GSTM2-C $n=12$	F157A $n=7$	Y160A $n=7$
Mean ± SEM	6.9 ± 0.72	8.6 ± 0.87	11.3 ± 1.84*	12.7 ± 3.2*

* $P < 0.05$.

significant ($P < 0.05$) inhibition of caffeine-activated Ca^{2+} release via ryanodine receptor channels (Fig. 3B). Although there was a marked depression of caffeine-induced Ca^{2+} release (slope a, Fig. 3B), there was no significant change in the baseline release in the presence of thapsigargin measured before caffeine addition (Fig. 3B, slope b and Table 1). In marked contrast to the wild type GSTM2-C, there was no inhibition of caffeine-induced Ca^{2+} release when 30 μM of either the F157A or Y160A mutant proteins were incubated with the SR. In both cases the release rate remained close to that seen under control conditions, or tended to be faster (Fig. 3B). The baseline release before caffeine addition was higher than control with both mutant proteins (Table 1). The average data in Fig. 3C shows that there was a reduction in the relative release rate when vesicles were incubated with 30 μM of the wild type GSTM2-C, but no change on average with either of mutants. The average control release rate was 47.1 ± 3.7 pmol of Ca^{2+}/mg/min.

3.3. Effects of wild type and mutant GSTM2-C on single RyR2 channels

3.3.1. Wild type GSTM2-2

Experiments were first conducted with the wild type GSTM2-2 to examine the effects of including 2 mM ATP in the cytoplasmic (*cis*) solution. ATP is an endogenous RyR2 ligand that enhances channel activity particularly in the presence of activating concentrations of cytoplasmic Ca^{2+} [17]. Previous experiments had not been performed in the presence of ATP and it was included here to more closely mimic the cytosolic solution within the cells and the extravesicular solutions used in the Ca^{2+} release experiments where ATP is required for Ca^{2+} pump activity during the initial phase of Ca^{2+} loading (see Section 2). The effect of the wild type GSTM2-C on channel activity was similar in the presence and absence of ATP (Fig. 4). As expected [17] the open times of RyR2 channels prior to addition of GSTM2-C were longer in the presence of 2 mM ATP than in its absence (compare Fig. 4A and C) and the average control open probability higher in the presence of ATP (Table 2).

The average data in Fig. 4B and D is expressed as relative open probability (i.e. $\log P_o c - \log P_o t$), to avoid the effects of the well documented variable gating between individual RyR channels under control conditions [18,19]. This heterogeneity of gating increases the variability of the average data and biases the average data towards the results obtained in the most active channels. The average "control" open probabilities obtained at +40 mV and at −40 mV before addition of the GST constructs are listed in Table 2. It is clear in Table 2 that there is no consistent difference between the average control P_o values obtained at +40 mV and −40 mV.

The effects of the wild type GSTM2-C added to the cytoplasmic side (*cis* solution) of RyR2 channels incorporated into lipid bilayers does appear to be voltage-dependent and the voltage-dependence is apparent in both the absence and presence of ATP. There is a strong decrease in channel activity at +40 mV, but little change in activity at −40 mV, and this is apparent in the channel recordings and in the graphs of average relative open probability (Fig. 4). In the presence of 2 mM ATP the relative values at +40 mV were significantly different from those at −40 mV with each GSTM2-C

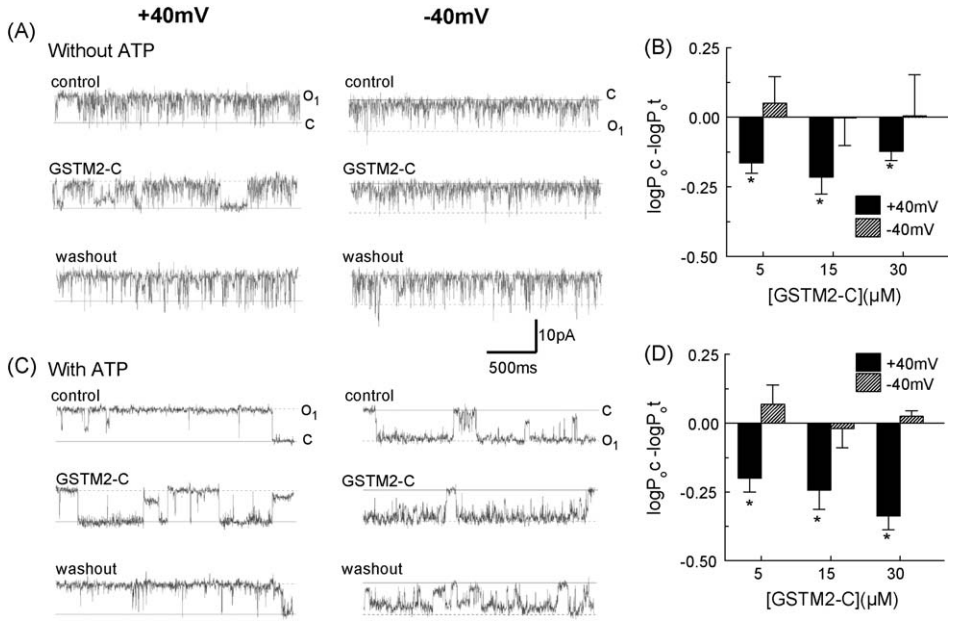

Fig. 4. Wild type GSTM2-C inhibits RyR2 channel activity in lipid bilayers at +40 mV in the absence and presence of 2 mM *cis* ATP. (A) and (C) show 3 s recordings of representative channel activity under each condition at +40 mV (left panel) and −40 mV (right panel). Channel opening is upward at +40 mV, from the closed level (solid line, *c*) to the maximum single channel current (broken line, o_1). At −40 mV, channel opening is downward from the closed level (*c*) to open levels o_1. The top record in each panel shows control activity before addition of GSTM2-C, the middle record shows activity after equilibration for >2 min in 15 μM GSTM2-C and the final record shows activity following perfusion of the *cis* chamber to remove GSTM2-C. In both the absence (A) and presence (C) of 2 mM ATP, the channel spends more time in the closed state in the presence of GSTM2-C than under control conditions or after washout. (B) and (D) show graphs of average relative P_o (i.e. the average of the P_o values for each individual channel relative the internal control for that channel) obtained in the absence (B) or presence (D) of ATP. The control value of 1 is indicated by the broken line. Data is shown for 5, 15 and 30 μM GSTM2-C as indicated, at +40 mV (filled bins) and −40 mV (cross-hatched bins). Asterisks (*) indicate values that are significantly different from control. Circles (•) indicate values at −40 mV that are significantly different from those at +40 mV at the same GSTM2-C concentration. Note the significant depression of channel activity caused by GSTM2-C at +40 mV only in both graphs.

Table 2
Average open probability (P_o) of the internal control for each channel in the particular experiments as listed in column 1. Control values for all three concentrations are included. This data is presented to indicate baseline parameter values of P_o, as average data relative to internal controls is presented in Figs. 4 and 5 to illustrate the effects of the GSTM2-C constructs on RyR2, to reduce anomalies introduced by the wide range of control values.

Experimental series	*n*	P_o +40 mV	P_o −40 mV
WT GSTM2-C without ATP	14	0.27 ± 0.06	0.22 ± 0.03
F157A without ATP	21	0.20 ± 0.02	0.29 ± 0.10
Y160A without ATP	16	0.38 ± 0.14	0.22 ± 0.04
WT GSTM2-C with ATP	20	0.42 ± 0.11	0.27 ± 0.07
F157A with ATP	14	0.39 ± 0.06	0.43 ± 0.03
Y160A with ATP	9	0.34 ± 0.04	0.24 ± 0.03

All values are the mean ± SEM.

concentration used. There was a significant decline in activity at +40 mV but no significant change in activity relative to control at −40 mV (Fig. 4B and D).

We have previously shown that the GSTM2-2 C-terminal constructs are active within a range of 3–30 μM [6]. The GSTM2-C concentration in the present experiments was increased progressively from 3 to 15 to 30 μM to ensure that the concentration used was close to saturating. Activity appeared to be the same at each concentration when the experiments were performed in the absence of ATP. There was a trend towards a greater decrease in activity in the presence of ATP with 30 μM wild type GSTM2-C than with 5 or 15 μM, so that activity may have decreased further had higher concentrations been added. This was not tested as it was not possible to easily concentrate the recombinant GSTM2-C constructs further. There was no significant difference between the relative changes in P_o in the absence or presence of ATP with 5 or 15 μM. The decrease in activity with 30 μM GSTM2-C was significantly greater in the presence of ATP (Fig. 4D) than in its absence.

In the context of GSTM2-C inhibiting these channels mainly at +40 mV, it is worth noting that a positive membrane potential would tend to develop across the SR membrane during Ca^{2+} efflux when positive charge is dumped onto the cytoplasmic side of the SR membrane. This is significant in the context of the potential use of these compounds as therapeutic agent (see Section 4).

3.3.2. Mutant GSTM2-C

The effects of both the mutant GSTM2-C proteins on single RyR2 Ca^{2+} channels were generally consistent with the results of the SR vesicle Ca^{2+} release study. In contrast to the effects of the wild type GSTM2C, neither of the Y157A or Y160A mutant proteins had any consistent effect on RyR2 activity when added to the cytoplasmic (*cis*) solution. This absence of an effect is evident in the individual channel recordings in the presence of ATP (Fig. 5A or C) and in the average relative open probabilities (Fig. 5B and D). The reason for this decline in activity in the one data set was not explored further. The general lack of an effect was not dependent on the presence of ATP as a similar lack of inhibition was also seen in the absence of ATP (Fig. 5E and F). The results in Fig. 5 with the two mutant proteins at +40 mV serve as a negative control for the strong effect of the wild type GSTM2-C shown in Fig. 4 at +40 mV, and indicate that the effect on RyR2 is specific for the wild type GSTM2-C sequence. The results also indicate that there are no intrinsic voltage-dependent changes in channel activity that develop as a function of time during the experiment.

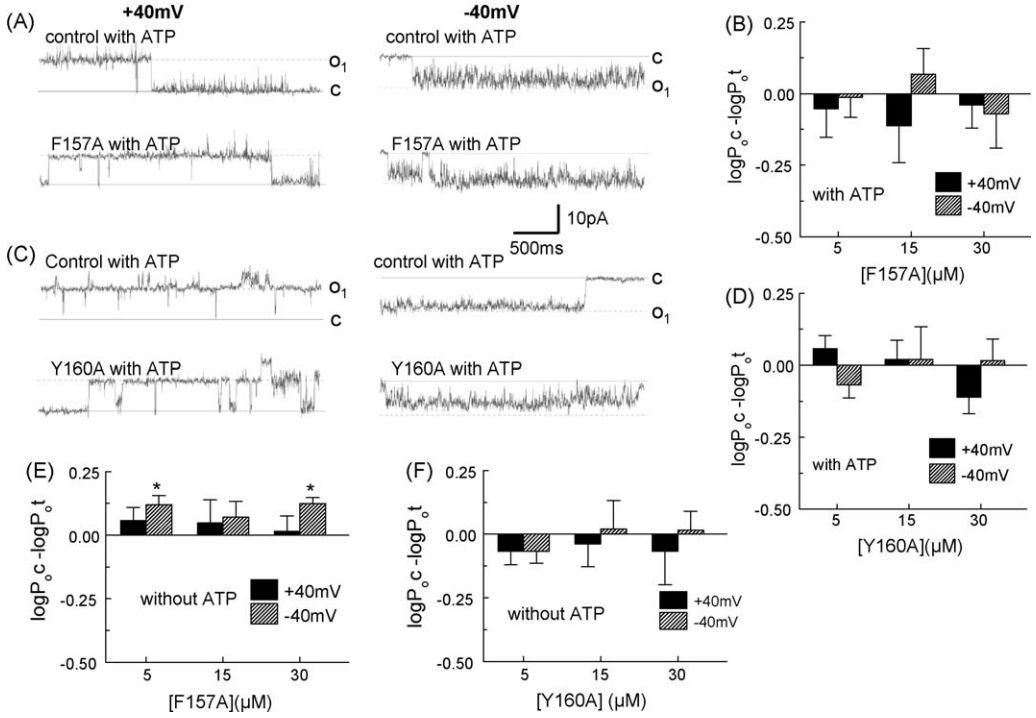

Fig. 5. Overall, neither the F157A nor the Y160A mutant GSTM2-C proteins inhibit RyR2 channel activity in lipid bilayers at +40 mV or −40 mV in the presence or absence of 2 mM *cis* ATP. (A) and (C) show 3 s recordings of representative channel activity under each condition at +40 mV (left panel) and −40 mV (right panel) in the presence of ATP. Channel opening is upward at +40 mV, from the closed level (solid line, *c*) to the maximum single channel current (broken line, o_1). At −40 mV, channel opening is downward from the closed level (*c*) to open levels o_1. The top record in each panel shows control activity before addition of the mutant GSTM2-C, the lower record shows activity after equilibration for >2 min in 30 μM of the mutant GSTM2-C. The lack of an effect of the mutants can be seen in recordings with both the F157A (A) and the Y160A (C) mutants. (B), (D), (E) and (F) show graphs of average relative P_o (i.e. the average of the log P_oc − log P_ot) values for each individual channel, where P_oc is the internal control for that channel) obtained with F157A (B) or Y160A (D). Data is shown for 5 μM, 15 μM and 30 μM mutant GSTM2-C as indicated, at +40 mV (filled bins) and −40 mV (cross-hatched bins). (B) and (D) show data obtained in the presence of ATP. (E) and (F) show data obtained in the same way from different channels in the absence of ATP.

4. Discussion

The results presented in this manuscript show clearly that mutation of two residues in helix 6 located in the C-terminal domain of GSTM2-2, prevents the C-terminal half of the protein from exerting its normal inhibitory action on Ca^{2+} release from cardiac SR through RyR2 channels and on cardiac RyR2 channel activity. This result confirms our previous hypothesis that the inhibitory element within GSTM2-C is centered around helix 6 [6] and is dependent on the tertiary structure of this region of the GSTM2-2 protein.

4.1. Effects of GSTM2-2 and the F157A, Y160A mutants on RyR2 channel activity

The Ca^{2+} release and single channel experiments show that mutation of either F157 or Y160 to alanine eliminates any inhibitory action of the C-terminal domain of GSTM2-2. It is most likely that the loss of activity is due to the structural change resulting from the substitutions, rather than the amino-acid substitutions (see discussion in the following section). An unexpected finding in this study was the voltage-dependence of the effect of the wild type GSTM2-C in the presence of ATP. There was a trend towards a difference between data at +40 mV and −40 mV in the absence of ATP and this trend became significant when the channel activity was amplified by ATP as it would be in the physiological in vivo situation. A positive potential would tend to develop across the SR membrane during Ca^{2+} efflux, either during systolic Ca^{2+} release or during diastole if the RyR is "leaky" as it is in heart failure. Thus the implication of the voltage-dependence is that the most significant effect of any GSTM2-C-terminal construct would be exerted during Ca^{2+} efflux and would be most effective during excess diastolic efflux. This is because modifications of the RyR activity during systole have only short term effects since there is an autocorrection in the overall Ca^{2+} signaling pathway to maintain a constant systolic Ca^{2+} transient [20]. Such autocorrection does not apply during diastole and it is a diastolic Ca^{2+} efflux that is responsible the delayed after depolarisations (DADS) that lead to arrhythmia. The results suggest that GSTM2-C constructs would have little inhibitory effect on the RyR2 channel during diastole in normal heart where there is very little Ca^{2+} efflux during diastole. Indeed, when Ca^{2+} efflux is small, there would be a tendency for a negative potential developing across the SR membrane with nett Ca^{2+} influx into the SR. The constructs would be most active during diastole when the RyR channel is abnormally leaky as in heart failure or with mutations which lead to polymorphic ventricular tachycardia [5]. These predictions will of course need to be tested in the future in the intact beating heart.

Interestingly, the full length GSTM2-2 protein did not demonstrate any significant voltage-dependence in its action on RyR2 channels [1]. Thus an implication of the voltage-dependence of the C-terminal construct is that any therapeutic agent based on its structure would exert an effect on the channel that might differ from the effect of the endogenous protein. The difference may mean that the inhibitory effect during systole would be greater than that during diastole. This would tend to conserve Ca^{2+} in the SR Ca^{2+} store and may help prevent arrhythmias arising from persistent Ca^{2+} release.

There was an increase in baseline leak in the presence of the mutants, but no effect on caffeine-induced Ca^{2+} release or on RyR2 activity in bilayers. This effect of the mutants was not explored further, since it did not appear in the activity of the wild type protein. The increase could have been due to a small effect of the mutants on Ca^{2+} leak through the Ca^{2+}-ATPase or on the interaction between thapsigargin and the Ca^{2+}-ATPase. On the other hand it may have been due to a weak non-specific effect of the mutants on unstimulated RyR2 activity since small increases in open probability were seen with the mutants in some cases (e.g. Fig. 4E).

4.2. Effects of the F157A, Y160A mutations on GSTM2-C structure

Our previous studies designed to identify a peptide that was responsible for the inhibition of RyR2 by GSTM2-2 suggested that although helix 6 within the C-terminal domain appeared to be a required component in all fragments of GSTM2-C that functioned as inhibitors of RyR2 [6], a peptide comprised of the helix 6 sequence alone was ineffective as an RyR2 inhibitor. As this individual peptide does not appear to form a helix we concluded that the inhibitory properties of the GSTM2-C domain and some of its multi helix fragments may be dependent on the conformation of the protein fold that is stabilized by helix 6 or dependent on the helical structure of the helix 6 sequence when it is stabilized by the surrounding helices [6]. The data presented here show that some single residue substitutions in helix 6 of the C-terminal domain of GSTM2-2 can destabilize the protein to such an extent that it cannot be expressed and purified from *E. coli*. This confirms that helix 6 plays a central role in stabilizing the folded structure of GSTM2-C and is consistent with the previous studies of [7] that showed that helix 6 contains a conserved motif that contributes to the global folding of GST proteins. Two other helix 6 mutations (F157A, Y160A) were less deleterious but their lack of an effect on Ca^{2+} release and RyR2 channel activity also confirmed that helix 6 plays a central role in maintaining the native fold of the C-terminal domain of GSTM2 or that the helical structure of the helix 6 residues is maintained by the surrounding helices. Although circular dichroism studies showed that these two mutations did not dissipate the overall helical secondary structure of GSTM2-C, significant changes in tryptophan fluorescence were observed indicating a modification in the fold in the proximity of trytophan residues at positions 146 and/or 214. This apparent change in structure associated with both the F157A and Y160A substitutions parallels the loss of their capacity to inhibit Ca^{2+} release and RyR2 channels. These data are consistent with two hypotheses. Firstly, that the binding of GSTM2-2 to RyR2 and the consequent inhibition of the ion channel and Ca^{2+} release from the SR is dependent on the recognition of the fold of the protein around helix 6. Or secondly, that the inhibitory action of GSTM2-2 is dependent on the helical structure of helix 6 residues that is stabilized by flanking helices in the C-terminal domain. The former possibility is most likely because helix 6 is buried, but the second might be possible if the position of helix 6 changes once GSTM2-C is influenced by the environment of the RyR protein.

GSTM2-C is one of the few selective inhibitors of RyR2 that does not influence skeletal muscle RyR1 activity [1,2,6]. Consequently GSTM2-C or a derivative is a potential therapeutic modulator of heart function through its ability to specifically inhibit cardiac ryanodine receptor Ca^{2+} channels. An advantage of using the GSTM2-C-terminal construct as a template for an RyR2 inhibitor is that the C-terminal construct has no GST enzyme activity. Thus its introduction into the cell would not have unwanted side effects that might be associated with altering the normal balance of GSTs within the cytosol. However this study shows that the development of such an inhibitor will require the delivery of a peptide or peptide mimetic of considerable complexity and is unlikely to be achieved by a small peptide unless we can show that the structure of helix 6 is itself important.

Acknowledgements

The authors are grateful to Suzy Pace and Joan Stivala for assistance with preparation of SR vesicles. The work was funded by

grants #268027 and #471462 from the Australian National Health and Medical Research Council.

References

[1] Abdellatif Y, Liu D, Gallant EM, Gage PW, Board PG, Dulhunty AF. The Mu class glutathione transferase is abundant in striated muscle and is an isoform-specific regulator of ryanodine receptor calcium channels. Cell Calcium 2007;41:429–40.
[2] Wei L, Abdellatif YA, Liu D, Kimura T, Coggan M, Gallant EM, et al. Muscle-specific GSTM2-2 on the luminal side of the sarcoplasmic reticulum modifies RyR ion channel activity. Int J Biochem Cell Biol 2008;40:1616–28.
[3] Laver DR, Baynes TM, Dulhunty AF. Magnesium inhibition of ryanodine-receptor calcium channels: evidence for two independent mechanisms. J Membr Biol 1997;156:213–29.
[4] Lamb GD, Stephenson DG. Effects of intracellular pH and [Mg^{2+}] on excitation-contraction coupling in skeletal muscle fibres of the rat. J Physiol 1994;478(Pt 2):331–9.
[5] Dulhunty AF, Beard NA, Pouliquin P, Casarotto MG. Agonists and antagonists of the cardiac ryanodine receptor: potential therapeutic agents? Pharmacol Ther 2007;113:247–63.
[6] Liu D, Hewawasam R, Pace SM, Gallant EM, Casarotto MG, Dulhunty AF, et al. Dissection of the inhibition of cardiac ryanodine receptors by human glutathione transferase GSTM2-2. Biochem Pharmacol 2009;77:1181–93.
[7] Aceto A, Dragani B, Melino S, Allocati N, Masulli M, Di Ilio C, et al. Identification of an N-capping box that affects the alpha 6-helix propensity in glutathione S-transferase superfamily proteins: a role for an invariant aspartic residue. Biochem J 1997;322(Pt 1):229–34.
[8] Baker RT, Catanzariti AM, Karunasekara Y, Soboleva TA, Sharwood R, Whitney S, et al. Using deubiquitylating enzymes as research tools. Methods Enzymol 2005;398:540–54.
[9] Chamberlain BK, Fleischer S. Isolation of canine cardiac sarcoplasmic reticulum. Methods Enzymol 1988;157:91–9.
[10] Laver DR, Roden LD, Ahern GP, Eager KR, Junankar PR, Dulhunty AF. Cytoplasmic Ca^{2+} inhibits the ryanodine receptor from cardiac muscle. J Membr Biol 1995;147:7–22.
[11] Ahern GP, Junankar PR, Dulhunty AF. Single channel activity of the ryanodine receptor calcium release channel is modulated by FK-506. FEBS Lett 1994;352:369–74.
[12] Dulhunty A, Gage P, Curtis S, Chelvanayagam G, Board P. The glutathione transferase structural family includes a nuclear chloride channel and a ryanodine receptor calcium release channel modulator. J Biol Chem 2001;276:3319–23.
[13] Board PG, Coggan M, Watson S, Gage PW, Dulhunty AF. CLIC-2 modulates cardiac ryanodine receptor Ca^{2+} release channels. Int J Biochem Cell Biol 2004;36:1599–612.
[14] Dulhunty AF, Pouliquin P, Coggan M, Gage PW, Board PG. A recently identified member of the glutathione transferase structural family modifies cardiac RyR2 substrate activity, coupled gating and activation by Ca^{2+} and ATP. Biochem J 2005;390:333–43.
[15] Jalilian C, Gallant EM, Board PG, Dulhunty AF. Redox potential and the response of cardiac ryanodine receptors to CLIC-2, a member of the glutathione S-transferase structural family. Antioxid Redox Signal 2008;10:1675–86.
[16] Raghunathan S, Chandross RJ, Kretsinger RH, Allison TJ, Penington CJ, Rule GS. Crystal structure of human class mu glutathione transferase GSTM2-2. Effects of lattice packing on conformational heterogeneity. J Mol Biol 1994;238:815–32.
[17] Kermode H, Williams AJ, Sitsapesan R. The interactions of ATP, ADP, and inorganic phosphate with the sheep cardiac ryanodine receptor. Biophys J 1998;74:1296–304.
[18] Copello JA, Barg S, Onoue H, Fleischer S. Heterogeneity of Ca^{2+} gating of skeletal muscle and cardiac ryanodine receptors. Biophys J 1997;73:141–56.
[19] Wei L, Gallant EM, Dulhunty AF, Beard NA. Junctin and triadin each activate skeletal ryanodine receptors but junctin alone mediates functional interactions with calsequestrin. Int J Biochem Cell Biol 2009;41:2214–24.
[20] Trafford AW, Diaz ME, Eisner DA. Stimulation of Ca-induced Ca release only transiently increases the systolic Ca transient: measurements of Ca fluxes and sarcoplasmic reticulum Ca. Cardiovasc Res 1998;37:710–7.